

MEASUREMENT OF THE LUMINOUS-REGION PROFILE AT THE PEP-II IP, AND APPLICATION TO e^\pm BUNCH-LENGTH DETERMINATION *

B. F. Viaud[†], Université de Montréal, Montréal, Quebec, Canada H3C 3J7

I. Narsky, California Institute of Technology, Pasadena CA 91125, U.S.A

W. Kozanecki, DAPNIA-SPP, CEA-Saclay, F91191 Gif-sur-Yvette, France

C. O'Grady, A. Perazzo, Stanford Linear Accelerator Center, Stanford CA 94309, U.S.A.

Abstract

The three-dimensional luminosity distribution at the interaction point (IP) of the SLAC B-Factory is measured continuously, using $e^+e^- \rightarrow e^+e^-$, $\mu^+\mu^-$ events reconstructed online in the *BABAR* detector. The centroid of the transverse luminosity profile provides a very precise and reliable monitor of medium- and long-term orbit drifts at the IP. The longitudinal centroid is sensitive to variations in the relative RF phase of the colliding beams, both over time and differentially along the bunch train. The measured horizontal r.m.s. width of the distribution is consistent with a sizeable dynamic- β effect; it is also useful as a benchmark of strong-strong beam-beam simulations. The longitudinal luminosity distribution depends on the e^\pm bunch lengths and vertical IP β -functions, which can be different in the high- and low-energy rings. Using independent estimates of the β functions, we analyze the longitudinal shape of the luminosity distribution in the presence of controlled variations in accelerating RF voltage and/or beam current, to extract measurements of the e^+ and e^- bunch lengths.

INTRODUCTION

Measuring the beam parameters at the interaction point (IP) of $e^+ - e^-$ colliders has historically been both essential and extremely challenging for accelerator builders. The high luminosity of the PEP-II B-factory [1], combined with the performance of the *BABAR* multilayer, two-sided silicon vertex tracker [2] and with advances in data acquisition and on-line processing capability, now makes it possible to reconstruct in real time a sufficient number of physics event vertices to characterize continuously the position and size of the luminous region in all three dimensions. These parameters provide feedback to the accelerator on the time scale of a few minutes, and are archived, together with other machine parameters, for long-term monitoring and offline characterization of the IP phase space.

LUMINOUS-REGION MONITORING

The elastic-scattering processes $e^+e^- \rightarrow e^+e^-$, $\mu^+\mu^-$ are chosen for our purposes, because of their simple, background-free topology and their low track multiplicity (which translates into faster event processing). Event data are collected on a farm of 32 Linux nodes. Based on

the level-1 trigger flags, subsets of events are redirected to eight monitoring CPUs that run the full *BABAR* tracking. Charged-particle trajectories are reconstructed using hits recorded in the *BABAR* Silicon Vertex Tracker (SVT) and Drift Chamber. The resulting track list is fed to a selection algorithm that retains the appropriate two-prong events.

The spatial coordinates of the retained event vertices are continuously histogrammed. The mean and standard deviation of these distributions, which reflect the centroid location and the r.m.s. size of the luminous region, are regularly updated and, after correction for experimental resolution, shipped to the accelerator control system [3]. The typical refresh period is 10 minutes, which at a luminosity of $9 \times 10^{33} \text{ cm}^{-2} \text{ s}^{-1}$ corresponds to 6000 accumulated events. The expected resolution on the luminous-centroid position is about $1 \mu\text{m}$, $0.5 \mu\text{m}$, and 0.1 mm in x , y and z respectively, as confirmed by the sample-to-sample scatter in the time history of the actual centroids (Fig. 1).

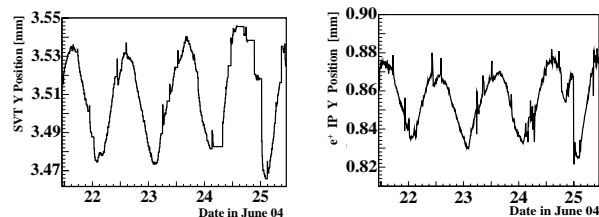


Figure 1: Time history of the vertical IP position. Left: vertical luminous centroid reported by *BABAR*. Right: y position of the e^+ beam at the IP, measured by the BPM's. The sine-like behavior is caused by day-night temperature variations.

The knowledge and long-term stability of the interaction-region (IR) orbit is crucial to ensure the reproducibility of the ring optics. The transverse IP position, in particular, is typically monitored using beam-position monitors (BPM's) located one or more quadrupoles away from the IP. Such a measurement is compared to the online *BABAR* data in Fig. 1. The IP-position variations reported by the BPMs is inconsistent in amplitude, and a couple of hours off in phase, compared to that reported by *BABAR*. This is attributed to the combination of several factors: lattice-modeling errors (which affect the transfer matrix from the BPMs to the IP); drifts in the BPM electronics; and mechanical motion (thermal expansion of mechanical supports, differential long-term

* Work supported in part by DOE Contract DE-AC02-76SF00515

[†] viaud@slac.stanford.edu

ground motion), that distorts, in a time-dependent manner, the relation between the beam position and angle at the IP and that at the BPMs. In contrast, the *BABAR* IP position directly measures the quantity of interest, on an absolute scale set by the extremely precise and stable mechanical structure of the SVT. It has proven a valuable tool to diagnose large thermally-induced motion in the IR, or to properly restore the horizontal IP position (to which the e^+ optics is rather sensitive) after long interruptions.

The longitudinal position z_c of the collision point, which ideally should coincide with that of the optical waists, is not directly measurable by accelerator techniques: only its relative variation averaged over the bunch train can be inferred from empirical, luminosity-driven adjustments of the RF-phase difference between the two rings. The SVT resolution is sufficient to routinely detect sub-mm changes in $\langle z_c \rangle_{train}$. The technique can be refined to measure the variation of z_c along the bunch train (Fig. 2), revealing systematic variations in longitudinal centroid location that depend on the bunch pattern and total beam current. The z_c spread with respect to the waist position is sometimes large enough to induce a noticeable luminosity loss and enhance the sensitivity to beam-beam effects.

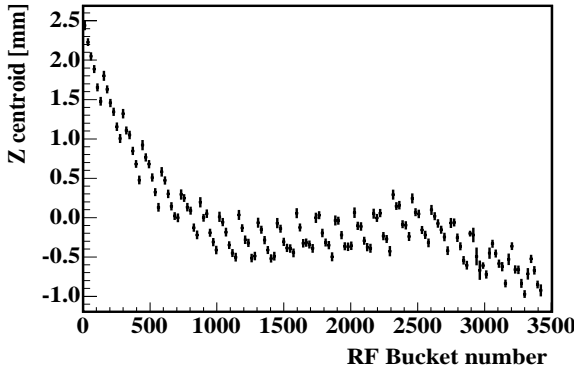


Figure 2: z_c -variation along the bunch train. The sharp transition at the beginning of the train reflects the RF-phase jumps caused by the 2% abort gap. The periodic structure is caused by variations in relative RF phase associated with the short gaps between the minitrains. The drift-chamber time resolution is sufficient to resolve individual bunches.

Under the assumptions of Gaussian beams and negligible x-y coupling, the transverse luminous size $\sigma_{x,y}^L$ is related to that of the e^\pm beams by $(\sigma_{x,y}^L)^{-2} = (\sigma_{x,y}^+)^{-2} + (\sigma_{x,y}^-)^{-2}$. Machine parameters typical of 2004 running are listed in Table 1. Because the actual vertical luminous size is much smaller than the vertexing resolution ($\sigma_{res} \approx 40 \mu m$), the apparent vertical luminous size directly measures that resolution, and must be taken into account when reporting the horizontal size [4].

An early application of luminous-size monitoring is presented in Ref. [5]: when the horizontal tunes were brought close to $\nu_x^\pm = 0.5$ in 2003, the combination of an actual reduction in β_x^{*-} , and of the dynamic- β effect in both rings,

Table 1: Single-beam IP parameters and luminous sizes.

Parameter	LER (e^+)	HER (e^-)
β_x^* / β_y^* (cm)	51 / 1.21	25 / 1.25
ϵ_x / ϵ_y (nm)	22 / 2.3	49 / 1.4
σ_x / σ_y (μm)	106 / 5.3	111 / 4.2
σ_x^L / σ_y^L (μm)	77 / 3.3 (low current, predicted)	
σ_x^L / σ_y^L (μm)	60 / 4.7 (high current, predicted)	
σ_x^L (μm)	67–69 (high current, measured)	

caused σ_x^L to shrink from about 90 to 67 μm . More recently, strong-strong beam-beam simulations [6] using the above-listed input parameters, predict a 25% reduction in horizontal luminous size associated with the dynamic- β effect. The data lie half-way between the low-current limit (based on estimated emittances and phase-advance measurements of β functions) and the high-current prediction (Table 1). Some of the simulation input parameters, however, are poorly known, making a quantitative comparison rather delicate. A direct measurement of the bunch-current dependence of σ_x^L is impractical, because it would require extensive running at very low luminosity.

BUNCH LENGTH MEASUREMENTS

The sensitivity of the luminous length to moderate changes in longitudinal parameters is illustrated in Fig. 3 (left). This suggests to measure the individual e^+ and e^- bunch lengths by analyzing the longitudinal shape of the luminosity distribution in the presence of known variations in RF voltage(s) and/or beam current(s), one beam at a time.

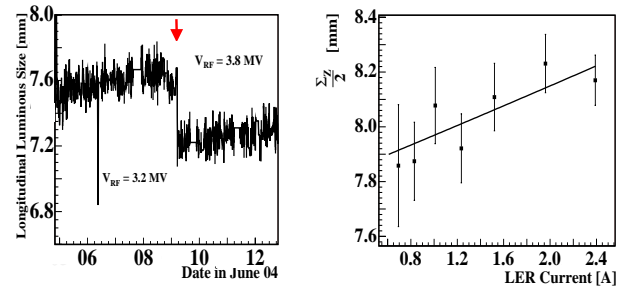


Figure 3: Left: history of the r.m.s. luminous length σ_z^L , before and after the LER RF voltage V_{RF}^+ was increased (arrow). The HER RF voltage V_{RF}^- remained constant. Right: e^+ -current dependence of the fitted value of $\Sigma_z/2$ ($\approx \sigma_z^L$) measured during a long coast-down. The line shows the fitted current-dependence (see text). The HER bunch length and the β functions are fixed in the fit.

The longitudinal luminosity distribution is given [7] by:

$$\mathcal{L}(z) = \frac{2N_+N_-}{\sqrt{(2\pi)^3 \Sigma_x \Sigma_y \Sigma_z}} \exp\left(\frac{-2(z - z_c)^2}{\Sigma_z^2}\right) \quad (1)$$

where $N_{+,-}$ are the e^\pm bunch populations, $\sigma_{z\pm}$ the bunch

lengths, $\Sigma_z = \sqrt{\sigma_{z+}^2 + \sigma_{z-}^2}$, and (with $t = x, y$)

$$\Sigma_t = \sqrt{\sigma_{t+}^{*2} \left(1 + \frac{(z - z_{t+})^2}{\beta_{t+}^{*2}} \right) + \sigma_{t-}^{*2} \left(1 + \frac{(z - z_{t-})^2}{\beta_{t-}^{*2}} \right)}$$

Here $\sigma_{ti}^* = \sqrt{\epsilon_{ti}^* \beta_{ti}^*}$ ($i = +, -$) is the horizontal or vertical size of beam i at the corresponding waist, z_{ti} is the longitudinal position of the waist, ϵ_{ti}^* and β_{ti}^* are, respectively, the corresponding emittance and the β function at the waist. The dominantly Gaussian shape of $\mathcal{L}(z)$ is modified, through its Σ_y dependence, by an hourglass factor function of $\beta_{y+,-}^*$ (the β_x^* dependence is negligible).

We first analyzed large samples ($\sim 0.5 - 2.5 \times 10^6$) of $\mu^+ \mu^-$ events recorded at two different settings of the LER RF voltage, with V_{RF}^- fixed. The known V_{RF} -dependence of the bunch length ($\sigma_z[V_2] = \sqrt{(V_1/V_2)} \sigma_z[V_1]$) provided the necessary extra constraint. The event selection criteria were tightened to minimize z -dependent acceptance, resolution and background effects. The measured vertex positions were corrected both for bucket-dependent offsets (Fig. 2), and for slow drifts in the average longitudinal luminous centroid. The results are summarized in Table 2. If the β functions are fixed to values measured using the betatron phase-advance method, the fitted e^- bunch length is consistent with the multibunch measurements of Ref. [8], but the fitted e^+ bunch length is substantially shorter and the fit χ^2 is very poor. If one allows β_y to float, the goodness of fit improves substantially, the resulting value of β_y^* is surprisingly large [9], but the bunch lengths decrease only slightly. Extensive studies were carried out to try and isolate the source of the poor goodness of fit (at fixed β_y^*) and of the apparent β_y^* bias (when fitted). The results are highly insensitive to variations in the event selection cuts, the portion of the bunch train included in the fit, or the assumed values of ring parameters such as waist positions, emittances and $\beta_{x+,-}^*$. The fitting procedure was validated on a parameterized simulation of $\mu^+ \mu^-$ events. To investigate the potential impact of beam-beam induced distortions of the luminous region, the fit was also applied to luminosity distributions produced by the beam-beam simulations of Ref. [6], both at nominal and at very low bunch currents (where distortions should be negligible). At all currents, the fitted bunch length at fixed β_y^* was consistent with the input value, and a similar upward “bias” was observed when floating the β -function. At this stage therefore, the origin of these systematic effects is unknown, but their impact on the bunch length measurement remains under 1 mm.

In a second experiment, we took advantage of a long coast-down during which the e^+ (e^-) current decayed from 2.4 (1.5) A to 0.65 (1.0) A. The luminous length exhibits a clear beam-current dependence (Fig. 3, right). As streak-camera measurements [8] suggest a strong (weak) dependence of the e^+ (e^-) bunch length on the corresponding total current, the data was fitted under the assumption

Table 2: Bunch length measurement varying V_{RF}^+ . The results are quoted at nominal currents ($I^+/I^- \approx 1.4/0.9$ mA/bunch), and at V_{RF}^+ (V_{RF}^-) = 3.8 (16) MV. The errors are statistical only. The total systematic uncertainty on σ_z is ± 1.1 mm. The last row shows the spectral measurements first, those using the streak camera second.

Parameter	LER (e^+)	HER (e^-)
β_y^* (mm, from phase advance)	10.6	10.3
σ_z (mm, fitted)	11.5 ± 0.4	12.0 ± 0.4
$\chi^2/D.O.F.$	30	
$\beta_{y+}^* = \beta_{y-}^*$ (mm, fitted)	16.1 ± 0.2	
σ_z (mm, fitted)	11.1 ± 1.1	11.1 ± 1.1
$\chi^2/D.O.F.$	3.5	
σ_z (mm, from [8])	13.2 – 15.5	11.6 – 11.1

that the σ_z^+ varied linearly with current, and that σ_z^- remained fixed to the value determined in the first experiment. The fit yields $\sigma_z^+ = 11.2 \pm 0.9$ mm at full current ($I_b^+ = 1.5$ mA/bunch), and $d\sigma_z^+/dI_b^+ = 0.84 \pm 0.37$ mm/(mA/bunch).

CONCLUSION

Online monitoring of the luminosity distribution using the *BABAR* detector has been providing routine diagnostics of transverse and longitudinal phase space parameters at the PEP-II IP. Offline analysis of $\mu^+ \mu^-$ events allows direct, non-invasive measurements of bunch lengths, and possibly of IP β functions, under nominal running conditions.

REFERENCES

- [1] J. Seeman *et al.*, “Performance of the PEP-II *B*-Factory Collider at Slac”, PAC’05, these proceedings.
- [2] B. Aubert *et al.* [*BABAR* Collaboration], “The *BABAR* detector”, Nucl. Instrum. Meth. A **479**, 1 (2002).
- [3] The algorithm also computes the directions of the luminosity-ellipsoid axes, but the y -resolution is too coarse to provide useful information on its $x - y$ tilt.
- [4] Even though σ_y^L is not directly measurable, it can still be extracted (at least in a single-ring collider) by using in addition the measured specific luminosity L_{sp} : $\sigma_y^L \sim \sigma_x^L \times L_{sp}$. Exploiting this method in a two-ring machine requires mild assumptions on the ratio of the e^+ and e^- beam sizes.
- [5] See Fig. 6 of: W. Kozanecki *et al.*, “Experimental Characterization of PEP-II Luminosity and Beam-beam Performance”, EPAC’04 (July 2004).
- [6] I. V. Narsky *et al.*, “Study of Beam-beam Effects at PEP-II”, EPAC’04 (July 2004).
- [7] M. Venturini and W. Kozanecki, SLAC-PUB-8699.
- [8] A. Fisher *et al.*, “Bunch-Length Measurements in PEP-II”, PAC’05, these proceedings.
- [9] Similar results are reported in J. Thompson *et al.*, these proceedings (MPPE057).